Cancer Letters 452 (2019) 191–202

Contents lists available at ScienceDirect

Cancer Letters

journal homepage: www.elsevier.com/locate/canlet

Original Articles

Protective autophagy decreases osimertinib cytotoxicity through regulation of stem cell-like properties in lung cancer

Li Li[a,1], Yubo Wang[a,1], Lin Jiao[a,1], Caiyu Lin[a], Conghua Lu[a], Kejun Zhang[b], Chen Hu[a], Junyi Ye[c], Dadong Zhang[d], Haiyan Wu[e], Mingxia Feng[a], Yong He[a,*]

[a] Department of Respiratory Disease, Daping Hospital, Army Medical University, Chongqing, 400042, China
[b] Department of Clinical Laboratory, Daping Hospital, Army Medical University, Chongqing, 400042, China
[c] Burning Rock Biotech, Guangzhou, 510300, China
[d] The Research and Development Institute of Precision Medicine, 3D Medicine Inc., Shanghai, 201114, China
[e] OrigiMed Co. Ltd, Shanghai, 201114, China

ABSTRACT

Osimertinib, a third-generation epidermal growth factor receptor - tyrosine kinase inhibitor (EGFR-TKI), shows great efficacy in EGFR-mutant non-small cell lung cancer (NSCLC); however, the resistance is inevitable. Osimertinib induces autophagy in NSCLC cells, but the role of autophagy in osimertinib resistance is not clear. We discovered that enhanced autophagy is associated with osimertinib resistance *in vitro* and *in vivo*. Inhibition of autophagy enhanced osimertinib cytotoxicity in both osimertinib-resistant and sensitive cells. Moreover, osimertinib-resistant cells exhibited stem cell-like properties, whereas autophagy inhibition decreased the stemness by downregulating the expression of SOX2 and ALDH1A1. Further, we found that knockdown of Beclin-1 inhibited the stem cell-like properties and restored osimertinib cytotoxicity. Osimertinib combined with chloroquine inhibited tumor growth more effectively than alone in xenograft mice. These results reveal that autophagy plays an adverse role in osimertinib cytotoxicity through inducing stem cell-like properties. Combination therapy of EGFR-TKI and autophagy inhibitor could provide a promising strategy to improve osimertinib cytotoxicity.

1. Introduction

In the last decade, treatment of non-small-cell lung cancer (NSCLC) has revolutionized from the traditional “one-size-fits-all” chemotherapeutic approach to molecular therapies targeting various oncogenic driver mutations. Osimertinib (AZD9291), as a third-generation irreversible epidermal growth factor receptor - tyrosine kinase inhibitor (EGFR-TKI), has shown significantly efficacy in advanced NSCLC patients with T790M [1,2],which is the most frequent acquired resistance mechanism after treatment with first-generation EGFR-TKI [3,4]. Moreover, osimertinib showed efficacy superior to that of first- or second-generation EGFR-TKIs in the first-line treatment of EGFR-mutant advanced NSCLC [5]. Despite high efficacy and low toxicity of osimertinib, patients will eventually acquire resistance and disease progression will inevitably occur [6]. Thus, innovative treatment strategies are urgently needed to overcome osimertinib resistance.

The mechanisms of osimertinib resistance are diverse and not fully understood. Emerging clinical data suggest that the underlying mechanisms to confer acquired resistance to osimertinib include: other EGFR mutations, C797S and L798I, which prevent drug binding [7,8]; bypassing of MET or ERBB2 signaling activation [9–12]; constitutive MAPK pathway activation by mutated KRAS or MEK [13]; amplification of EGFR wild-type alleles [14]. However, a significant percentage of patients likely develop resistance by as yet unknown mechanisms. Therefore, it is of great significance to investigate the potential mechanism and new treatment regimens that may reverse osimertinib resistance or enhance osimertinib efficacy.

Autophagy is an evolutionarily conserved catabolic process involving the degradation of cytoplasmic constituents, and the recycling of long-lived or aggregated proteins [15]. In multiple tumor cells, autophagy is upregulated during adverse conditions, including chemoradiotherapy or a nutrient-deficient environment, promoting tumor cell survival; thus, autophagy may be considered a potential mechanism of drug resistance [16–18]. In NSCLC treated with EGFR-TKI, autophagy is a double-edged sword contributing to both cell survival and death. Reduced autophagy was related to resistance to erlotinib therapy [19]. On the other hand, several studies have shown that treatment of erlotinib or afatinib induced autophagy and inhibition of autophagy improves the anti-tumor activity of these drugs in lung adenocarcinoma [20,21]. Moreover, the pro-cell survival and pro-cell death roles of autophagy can be switched by adding gefitinib at an early time of hypoxia or by re-activating EGFR at a later time of hypoxia in cancer cell

* Corresponding author.
E-mail address: heyong8998@126.com (Y. He).
[1] These authors contributed equally to this work.

https://doi.org/10.1016/j.canlet.2019.03.027
Received 29 November 2018; Received in revised form 4 March 2019; Accepted 10 March 2019

lines [22]. Therefore, more works are needed to more comprehensively understand the role of autophagy in EGFR-targeted therapy for NSCLCs. As a third-generation EGFR-TKI, osimertinib has a different chemical structure and different potential resistance mechanisms comparing to first- or second-generation EGFR-TKIs. Previously, osimertinib was found to induce autophagy in osimertinib-sensitive cells, while autophagy was only suggested to be an accompanying effect [23,24]. It is unknown whether autophagy plays a role in osimertinib resistance, and whether inhibition of autophagy may restore osimertinib sensitivity.

In this study, we aim to understand the role of autophagy in osimertinib resistance and characterize the possible resistant mechanisms. Herein, we demonstrated that autophagy was enhanced in osimertinib-resistant cells as well as in lung cancer patients with resistance to osimertinib. We further showed that autophagy played as an negative regulator in osimertinib efficacy. Therefore, inhibition of autophagy can be explored as a new therapeutic approach to enhance osimertinib sensitivity in NSCLC patients.

2. Materials and methods

2.1. Cell lines

Human lung cancer cell lines PC-9 and gefitinib-resistant PC-9GR were generously provided by Prof. J. Xu and Dr. M. Liu (Guangzhou Medical University, China). H1975 cells were from the American Type Culture Collection (ATCC). To establish the corresponding osimertinib-resistant cell lines, the parental cells were first treated with osimertinib at the concentration of IC_{50} for 2 weeks. The cells were then treated for another 3 weeks with a higher concentration sufficient to kill nearly all parental cells. The remaining resistant clones were seeded single cell per well and cultured continuously in the presence of osimertinib. Cell lines were cultured in RPMI-1640 (Hyclone) with Earle's salts, supplemented with 10% FBS (Gibco), 2 mmol/L L-glutamine (Gibco), 100U/ml penicillin (HyClone), and 100 μg/mL streptomycin (Hyclone) at 37 °C, with 5% CO_2 and 90% humidity.

2.2. Reagents and antibodies

Osimertinib (Tagrisso) was provided by Astra Zeneca. Spautin-1 (S7888) and rapamycin (S1039) were purchased from Selleck. Chloroquine (C6628) was from Sigma-Aldrich. Antibodies against LC3II (#12741S), SQSTM1/p62 (#8025S), Beclin-1 (#3495S), phospho-(Ser93)-Beclin-1 (#14717S), phospho-(Ser2448)-mTOR (5536S), SOX-2 (#3579S), ALDH1A1 (#36671S), GAPDH (#2118S) were from Cell Signaling Technology.

2.3. Cell growth assays

The MTT cell proliferation assay was performed as previously described [25]. Briefly, 2×10^3 cells/well were seeded in 96-well plates. Twenty-four hours after seeding, the cells were treated with either osimertinib or dimethyl sulfoxide (DMSO). Absorbance was measured 72 h after treatment. All experiments were repeated for at least three times. Cell proliferation was also assessed by the Ki67 incorporation assay with a Ki67 labeling and detection kit (BM2889, Boster). Briefly, cells were treated as indicated for 48 h, incubated for 6 h with Ki67 at 1:200 dilution, and fixed. Fixed cells were counterstained with 4′, 6-diamidino-2-phenylindole (DAPI) and observed under a fluorescence microscope.

2.4. Colony-formation assay

Briefly, 500 cells were resuspended in culture medium and seeded in six-well plates. Osimertinib was added to culture medium (10 nM for PC-9, PC-9OR, PC-9GR, PC-9GROR cells, and 100 nM for H1975 and H1975OR cells). After 14 days of culture, the cells were fixed with 4% paraformaldehyde and stained with 0.1% crystal violet. Colonies with a diameter greater than 1 mm were counted. Samples were assayed in triplicate.

2.5. Pulmosphere formation assay

For tumor pulmosphere formation, 1×10^3 tumor cells were seeded in non-adhesive 6-well plates. One week after seeding, cell spheres characterized by tight, spherical, non-adherent colonies of more than 90 μm in diameter were observed. All experiments were repeated at least three times.

2.6. Flow cytometry

For CD133 and CD44 staining, 10^6 cells were incubated with 10 μl each of anti-CD133-PE (AC133 clone; Miltenyi Biotech) and anti-CD44-FITC (REA690 clone; Miltenyi Biotech) antibodies diluted in 100 μl of staining solution for 15 min at 4 °C. Then, 400 μl of buffer was added, and samples were analyzed with the CytExpert software (Beckman Coulter, USA).

2.7. Transmission electron microscopy (TEM)

The cells were pre-fixed with 2.5% glutaraldehyde in 0.1M PBS (pH 7.4) for 2 h at room temperature, and post-fixed with 1% osmium tetroxide for 2 h. The samples were dehydrated step-wise in increasing concentrations of ethanol (50%, 70% and 100%) and acetone, and finally embedded in Araldite. Fifty to 60 nm sections were prepared on a LKB-I ultramicrotome and transferred to copper grids, post-stained with uranyl acetate and lead citrate, and examined by Gatan JEM-1400 plus transmission electron microscope.

2.8. Whole-exome sequencing

Whole-exome sequencing libraries were prepared with 3 mg DNA. Exomes were captured using the NimbleGen SeqCap Non-Standard Material 110823-HG19-BEx-L2R-D03-EZ for whole exome sequencing, and libraries were hybridized to custom-designed biotinylated oligonucleotide probes (Roche NimbleGen, USA) covering the target region sequence for target-capture sequencing. DNA sequencing was carried out on a HiSeq Sequencing System (Illumina, CA) with 2 × 151-bp and 2 × 76-bp paired-end reads for WES and target-capture sequencing, respectively. Raw sequencing reads were filtered to obtain clean reads, which were then aligned to human genome assembly HG19 with Burrows-Wheeler Aligner (BWA) [26]. Reads with multiple mapping loci in the genome, and those with more than three mismatches, more than one gap, or a gap of more than 20 bases long were removed. Reads harboring an Indel within 5 bp of the fragment ends were removed. Duplicated reads derived from PCR amplification were marked with Picard tools (http://broadinstitute.github.io/picard/). Local realignments and base-quality recalibrations were performed with the GATK software (https://www.broadinstitute.org/gatk/).

2.9. Measurement of autophagic flux

To measure autophagic flux, pBABE-EGFP-mCherry-MAP1LC3B (Addgene plasmid#: 22418) plasmid was obtained from Addgene and detailed methods was described previously [27,28]. PC-9GR and PC-9GROR cells were transiently transfected with the plasmid using Lipofectamine 2000 for 6 h and then replaced with fresh medium. Fluorescent images were collected every 12 h interval until 72 h using ImageXpress Micro XLS Widefield High-Content Screening System (Molecular Devices). Autophagic flux was determined by the presence of yellow puncta (the overlap of red and green fluorescence signal), and red puncta (the quenching of EGFP in the acidic environment of lysosomes).

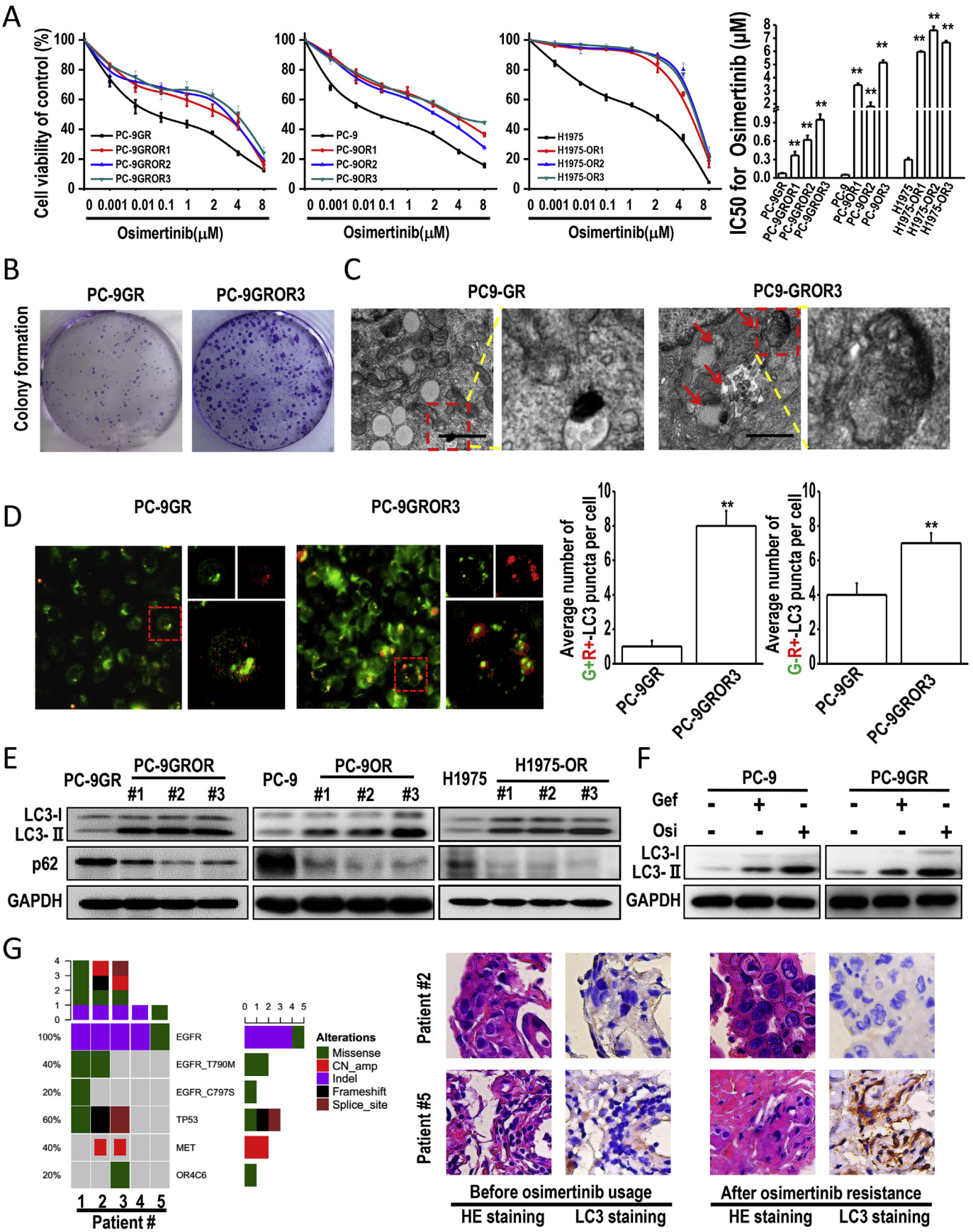

(caption on next page)

Fig. 1. Enhanced autophagy was found in osimertinib-resistant cells and patients with acquired resistance to osimertinib. (A) MTT assay for parental PC-9GR, PC-9, H1975 cells and their corresponding resistant cells treated with increasing concentrations of osimertinib for 48 h. Experiments were performed in triplicate, and data are mean ± SEM. Histogram shows IC_{50} values in the indicated groups (**p < 0.01 by Student's *t*-test). (B) Colony formation assay of resistant PC-9GROR3 cells and parental PC-9GR cells under osimertinib treatment. (C) Micrographs obtained by transmission electron microscopy showing enhanced autophagosomes in resistant cells compared with parental PC-9GR. Magnification, 4×10^4. Scale bar: 1 μm (D) The level of autophagy flux is increased in PC-9GROR3 cells. Representative images of mCherry-EGFP-LC3 vector were shown by fluorescent detection. The level of autophagy flux in PC-9GROR3 cells were increased compared with that in PC-9GR cells. Quantitative analysis of the number of yellow autophagosomes and red autolysosomes. **P < 0.01. (E) Upregulated protein levels of LC3II and downregulated level of p62 was found in PC-9GROR, PC-9OR and H1975-OR cells. (F) Osimertinib treatment induced autophagy to a much greater extent than that of gefitinib in both PC-9 cells and PC-9GR cells. Gefitinib, 10 nM in PC-9 cells and 4 μM in PC-9GR cells; osimertinib, 20 nM in PC-9 cells and 10 nM in PC-9GR cells. The level of LC3 was examined using Western blot. (G) Overall mutation spectrum of the 5 patients. Different colors present different types of baseline mutation. The top bar demonstrated the number of mutations detected in an individual patient. The side bar stands for the number of patients harboring the corresponding mutation. Immunohistochemical staining results for LC3 and hematoxylin-eosin staining in paired tumor sections from 2 patients (before osimertinib treatment and after osimertinib resistance). Positive staining was seen in patient # 5 after osiemrtinib treatment. (For interpretation of the references to color in this figure legend, the reader is referred to the Web version of this article.)

2.10. Western blot

Cells were washed with PBS twice, lysed for 30 min at 4 °C in RIPA buffer (Sigma-Aldrich, France) and harvested by scraping. The crude protein lysates were spun at 12000 × *g* for 15 min at 4 °C to remove cell debris. BCA assay was used to estimate the protein concentration. Equal amounts of protein per sample were boiled, loaded onto SDS-PAGE and allowed to separate for 2 h at 110 V. Separated proteins were transferred onto PVDF membranes (Roche, Switzerland) for 90 min at 200 mA. Membranes were blocked with 5% bovine serum albumin (BSA) for 1 h at room temperature and incubated with primary antibodies overnight at 4 °C. Subsequently, the membranes were washed and incubated accordingly with 0.02 μg/ml horseradish peroxidase (HRP)-conjugated goat anti-rabbit or anti-mouse IgG (Cell Signaling Technology, USA) for 1 h, and visualized with ChemiDoc Touch System (Bio-Rad, USA).

2.11. siRNA transfection

Small interfering RNAs (siRNAs) were synthesized by Shanghai GenePharma Co., Ltd. (Shanghai, China). For the evaluation of efficacy, PC-9OR cells cultured in 6-well plates were transfected with either 80 pmol siRNA or negative control siRNA (siNC) using Lipofectamine RNAiMAX (Thermo Fisher Scientific), following the manufacturer's instructions. At 72 h post-transfection, knockdown efficiency was determined by examining endogenous protein expression by Western blot.

2.12. Xenografts

Methods for xenograft implantation were described previously [29]. All experiments involving animals were approved by the Ethics Committee of the Army Medical University. The animals were maintained in individual ventilated cages in compliance with institutional guidelines. To briefly describe the xenograft implantation, 2×10^6 PC-9GR cells were injected subcutaneously into the back, next to the left forelimb of 6-week-old female BALB/c A-nu mice (Laboratory Animal Center of Army Medical University, Chongqing, China), which all developed tumors of ~30 mm^3 within 5–7 days. The mice were then randomly assigned to 4 groups (8 mice/group), and treated with chloroquine (CQ, 100 mg/L), osimertinib (20 mg/L), combined CQ and osimertinib, or drinking water (vehicle) alone. The tumor volume was calculated as (length × $width^2$)/2, and measured twice a week. The animals were monitored for 4 weeks until euthanasia. For immunohistochemistry assay, tumor-bearing mice in each group were sacrificed after 4 weeks of drug administration for the harvest of tumors.

2.13. Statistical analysis

Statistical analysis was performed by GraphPad Prism 5 and the data were presented as mean ± S.E.M. The two-tailed Student' s *t*-test was used to compare multiple sets of data. P < 0.05 was considered to be statistically significant.

3. Results

3.1. Enhanced autophagy is strongly associated with osimertinib resistance in vitro and in vivo

In order to represent the clinical scenario of osimertinib use, three cell lines were selected for the experiments. PC-9 cells harbor EGFR 19del and sensitive to first-generation EGFR-TKIs, while PC-9GR cells harbor EGFR T790M and have an acquired resistance to the first-generation EGFR-TKI gefitinib, and H1975 cells harbor a de novo T790M and primary resistance to gefitinib. In order to study the role of autophagy in osimertinib resistance, osimertinib-resistant PC-9, PC-9GR and H1975 cell lines were generated using the single-colony selection method. The origin of the parental cells was confirmed by short tandem repeat (STR) loci assay. The resulting osimertinib-resistant cells, referred to as PC-9OR, PC-9GROR and H1975-OR, displayed similar morphologic features as their respective parental cells (Fig. S1A). Osimertinib resistance of the cell lines were then evaluated by examining the survival of all 3 cell lines under varied concentrations of osimertinib. Results from the MTT assay demonstrated that the osimertinib-resistant cell lines survived even under high osimertinib concentration, with a marked increase in IC_{50} as compared to the parental cells (Fig. 1A). Consistently, osimertinib-resistant cells proliferated under osimertinib pressure as compared to the parental cells (Fig. 1B and Fig. S1B). These results demonstrate that the cell lines we have generated for the succeeding experiments were highly resistant to osimertinib.

To explore potential resistance mechanisms, DNA isolated from parental and resistant cells was subjected to whole exome sequencing. Several genetic alterations potentially relevant to osimertinib resistance were identified (Fig. S1D). Appearance of an *EGFR* amplification and loss of T790M were identified in the PC-9GROR3 cells. Amplifications in *MET* and *BRAF* were detected in H1975-OR cells and H1975-OR1 cells, respectively. However, no new mutation was found in PC-9OR cells. These results indicated that diverse mechanisms may exist in osimertinib resistance.

We next assessed whether a common mechanism underlies osimertinib resistance. To investigate whether autophagy is induced in osimertinib-resistant cell lines, we used transmission electron microscopy to identify the accumulation of autophagosomes. Transmission electron microscopy remains to be the most accurate method to identify autophagy in cells. Double-membrane autophagosomes can be morphologically distinguished from single-membraned autolysosomes judged by the difference in electron density. In osimertinib-resistant PC-9OR3, PC-9GROR3 and H1975-OR3 cells, more organelles were encapsulated in autolysosomes as compared to their respective parental cells (Fig. 1C and Fig. S1C).

We further examined the relative levels of autophagic flux using transient transfection of mCherry-EGFP-LC3 in PC-9GR and PC-

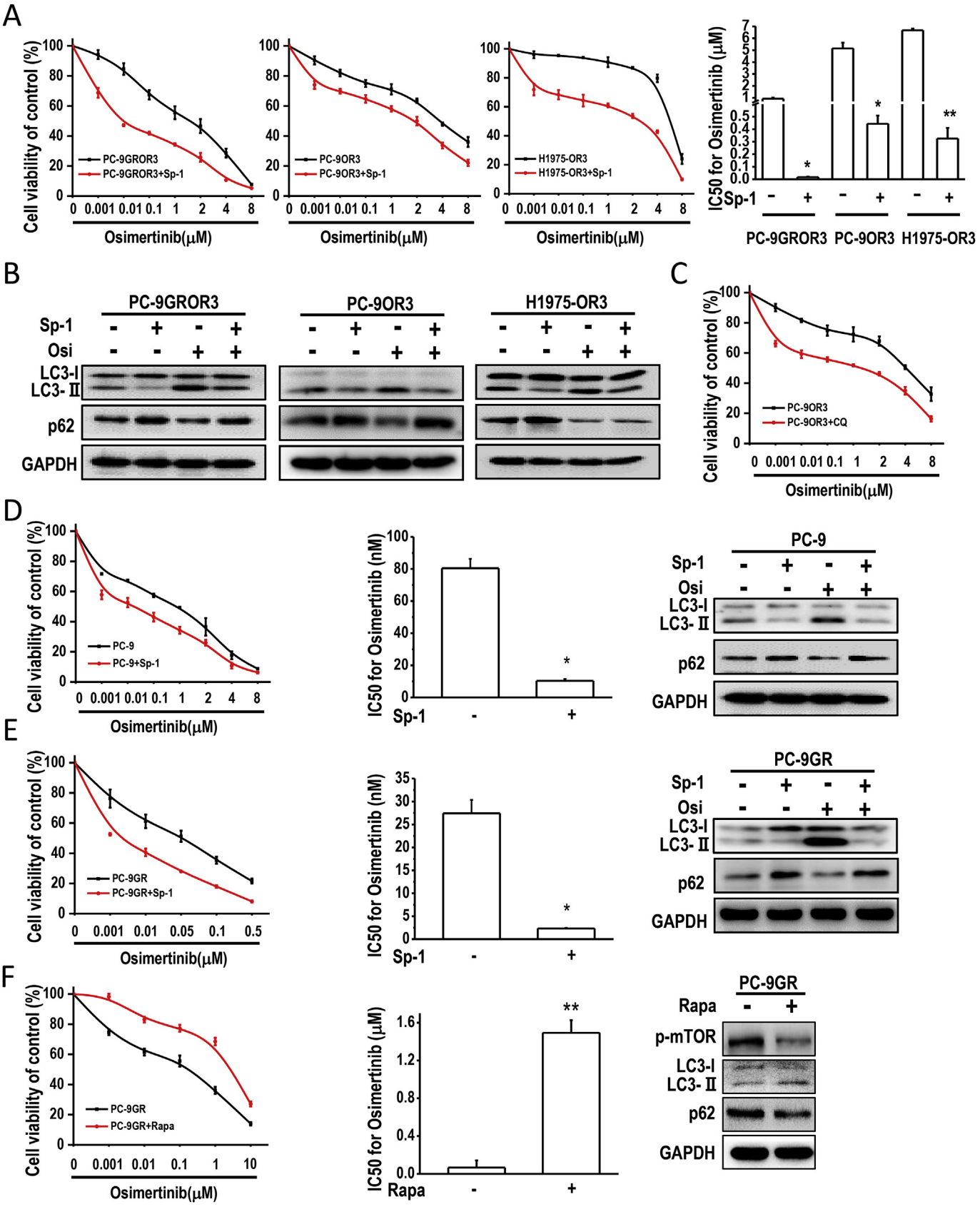

(caption on next page)

Fig. 2. Enhanced autophagy determines osimertinib resistance (A) MTT assay for PC-9GROR3, PC-9OR3 and H1975-OR3. Cells were treated with osimertinib with or without autophagy inhibitor, spautin-1 (10 μM) for 72 h. Experiments were performed in triplicate, and data are mean ± SEM. Histogram shows IC_{50} values in the indicated groups (*p < 0.05, **p < 0.01 by Student's *t*-test). (B) Western blot analysis of cells treated by spautin-1 (10 μM) for 48 h. (C) Cell viability MTT assay for PC-9-derived resistant cells treated with indicated concentration of osimertinib with or without CQ (10 μM) for 48 h. (D) Cell viability MTT assay for PC-9 cells treated with indicated concentration of osimertinib with or without spautin-1 (10 μM) for 48 h. Experiments were performed in triplicates and results are shown as mean ± SEM. Histogram shows IC_{50} values in the indicated groups (*p < 0.05 in Student's *t*-test). Western blot analysis of PC-9 cells treated by spautin-1 (10 μM) for 48 h. (E) Cell viability MTT assay for PC-9GR cells treated with indicated concentration of osimertinib with or without spautin-1 (10 μM) for 48 h. Experiments were performed in triplicates and results are shown as mean ± SEM. Histogram shows IC_{50} in the indicated groups (*p < 0.05 in Student's *t*-test). Western blot analysis of PC-9GR cells treated by spautin-1 (10 μM) for 48 h. (F) Cell viability MTT assay for PC-9GR cells treated with the indicated concentrations of osimertinib with or without rapamycin (500 nM) for 48 h. Experiments were performed in triplicate, and data are mean ± SEM (**p < 0.01 by Student's *t*-test). Western blot assessment of PC-9GR cells treated with rapamycin for 48 h. Rapa, rapamycin.

9GROR3 cells. With mCherry-EGFP-LC3, autophagosomes are visualized by the presence of yellow puncta indicated by the overlap of red and green fluorescence signals, while autolysosomes are visualized by the presence of red puncta depicted by the quenching of EGFP in the acidic environment of lysosomes. Accordingly, expression of the mCherry-EGFP-LC3 fusion protein in osimertinib-resistant PC-9GROR cells exhibited both yellow ($mCherry^+EGFP^+$) and red ($mCherry^+EGFP^-$) puncta throughout the cytoplasm, indicating the presence of autophagosomes and autolysosomes, respectively (Fig. 1D). The number of autophagosomes and autolysosomes in the osimertinib-resistant PC-9GROR cells was significantly increased as compared to the parental PC-9GR cells. Consistently, immunoblotting results also demonstrate an increase in conversion of LC3I to LC3II causing an accumulation of LC3II and decrease in p62 in osimertinib-resistant PC-9GROR, PC-9OR and H1975-OR cells (Fig. 1E). Taken together, these results indicate that the autophagic flux levels are higher in osimertinib-resistant cells.

We next interrogated whether autophagy can be induced by osimertinib or gefitinib treatment in osimertinib-sensitive parental cells. Interestingly, osimertinib-sensitive cells displayed a striking difference in gefitinib and osimertinib-induced autophagy. Osimertinib treatment resulted in an increased accumulation of LC3II than gefitinib treatment in both osimertinib-sensitive parental PC-9 and PC-9GR cells, suggesting that osimertinib is more able to induce increase in autophagy than gefitinib (Fig. 1F).

Based on our *in vitro* observations that osimertinib-resistant cells have increased autophagy, we then investigated whether NSCLC patients who developed osimertinib resistance would exhibit an enhanced autophagy. A retrospective analysis was performed by enrolling NSCLC patients who had developed osimertinib resistance from August 2015 to February 2018 in our hospital. Prior to treatment with osimertinib, all of these patients acquired EGFR T790M-mediated resistance to first-generation EGFR-TKI. The mutation spectra from the 5 patients demonstrated the disappearance of EGFR T790M in patients 3, 4 and 5, the co-occurrence of EGFR T790M and C797S in patient 1, and presence of *MET* amplification in patients #2 and #3 (Fig. 1G). Immunohistochemical staining of LC3 in tumor tissue samples from 5 patients before osimertinib treatment showed low LC3 expression. However, after developing osimertinib resistance, marked increase in LC3 expression was detected in 3 patients (Patients #1, #4 and #5, and images from all 5 patients were shown in Fig. 1G and Fig. S2). Taken together, these results strongly indicate that autophagy was a common mechanism underlies osimertinib resistance.

3.2. Protective autophagy mediates osimertinib resistance in vitro

Next, we used pharmacologic inhibition of autophagy to further understand the role of autophagy in osimertinib resistance. Two potent autophagy inhibitors, spautin-1 (Sp-1) and chloroquine diphosphate salt (CQ) were used. Treatment of PC-9OR, PC-9GROR and H1975OR cells with Sp-1 resulted in the re-sensitization of these resistant cells to osimertinib (Fig. 2A). Moreover, Sp-1 treatment in these cells also resulted in the suppression of autophagy, as shown by a decrease in the conversion of LC3I to LC3II and increased p62 protein expression (Fig. 2B). Consistently, CQ treatment also resulted in the re-sensitization of PC-9OR3 cells to osimertinib (Fig. 2C), with a corresponding decrease in the conversion of LC3I to LC3II indicating a decrease in autophagy levels (Fig. S3A). Taken together, these results indicate that inhibition of autophagy re-sensitized the cells to osimertinib, further indicating that the enhanced autophagy in osimertinib-resistant cell lines can be reversed by pharmacologic inhibition of autophagy.

We also found that treatment of osimertinib-sensitive parental cells, PC-9 and PC9-GR cells, with Sp-1 abolished osimertinib-induced autophagy and significantly increased osimertinib sensitivity in both cell lines (Fig. 2D and E). Similar results were obtained with CQ treatment (Fig. S3B). These results demonstrated that the autophagy induced by osimertinib in osimertinib-sensitive cells can be reversed by pharmacologic inhibition of autophagy, thus enhancing osimertinib efficacy.

Since autophagy is inhibited by the mammalian target of rapamycin (mTOR), we then used rapamycin, an inhibitor of mTOR to investigate whether rapamycin-induced autophagy could affect osimertinib sensitivity. Indeed, pharmacologic induction of autophagy of osimertinib-sensitive PC-9GR cells with rapamycin resulted in decreased osimertinib sensitivity (Fig. 2F), and induction of autophagy were confirmed by the increased conversion of LC3I to LC3II and corresponding decrease in p62 expression. Collectively, from our data we conclude that autophagy plays an important role in osimertinib sensitivity. These results further suggest that pharmacological inhibition of autophagy enhanced osimertinib efficacy.

3.3. Osimertinib-resistant cells exhibit typical stem cell-like properties

We next asked how autophagy regulates osimertinib resistance. Cancer stem-like cells, by contributing to tumor heterogeneity, have been implicated to cause disease relapse and drug resistance [30]. Moreover, through reduction of cancer stem cell activity, autophagy was reported to potentiate the tumoricidal effect of gemcitabine in pancreatic cancer [31]. Our observations on the high proliferation and colony forming ability in osimertinib-resistant cells led us to question whether these resistant cells display stem cell-like properties and whether these properties have a role in osimertinib resistance. As expected, osimertinib-resistant cells PC-9GROR, PC-9OR and H1975-OR cells displayed increased pulmospheres in terms of number and size, as compared to the osimertinib-sensitive parental PC-9GR, PC-9 and H1975 cells, respectively (Fig. 3A). CD133 and CD44 are regarded as specific markers for stem-like cells in lung cancer [32–34]. FACS analysis revealed that CD133-and CD44-positive cell populations in all osimertinib-resistant PC-9OR, PC-9GROR and H1975-OR cells were higher than their parental cells (Fig. 3B). In addition, it was reported that the transcription factor SOX2 and aldehyde dehydrogenase (ALDH) play major roles in stem-like NSCLC cells [35–37], both of which are implicated in conferring drug resistance to tyrosine kinase inhibitors [38,39]. Consistent with these reports, higher protein expression of SOX2 and ALDH1A1 was observed in most osimertinib-resistant cells as compared to their parental cells (Fig. 3C). Of note, the level of ALDH1A1 showed little change between PC-9 cells and PC-9OR #1 and #2 cells, while SOX2 levels were significantly higher in both cell lines. Taken together, these results demonstrated that osimertinib-resistant

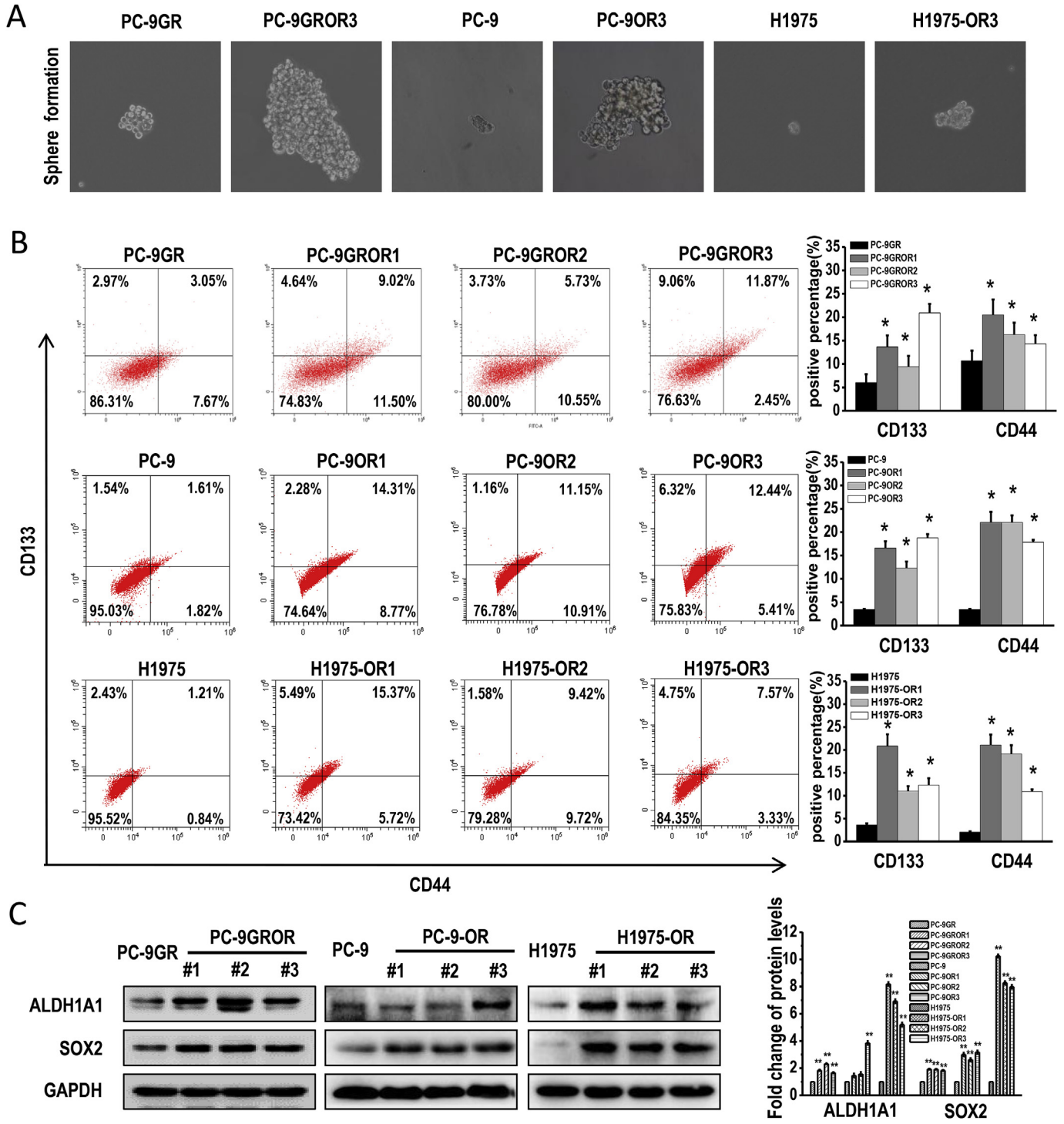

Fig. 3. Enhanced stem cell-like properties in osimertinib-resistant cells. (A) Osimertinib resistant cells show robust stem-cell like properties as determined by pulmosphere formation assays. Parental and resistant cells were diluted to single cells per well in 6-well low-adhesion plates. Micrographs of spheres formed after 7 days. (B) Increased proportions of CD133/CD44 positive cells were found in osimertinib-resistant PC-9GROR, PC-9OR and H1975-OR cells, as detected by flow cytometry using anti-CD133-FITC and CD44-PE antibodies. Top left and top right quadrants represent CD133 positive populations, while top right and lower right are CD44 positive populations. The bar chart shows percentages in various groups (n = 3, *p < 0.05 by Student's *t*-test). (C) Western blot showing the expression levels of the potential stem markers ALDH1A1 and SOX2 in osimertinib-resistant cells. Quantification of blots is shown. (**p < 0.01 by Student's *t*-test).

cells exhibit stem cell-like properties including enhanced pulmosphere formation ability, higher CD133/CD44 enrichment and upregulated expression of SOX2 and ALDH1A1.

3.4. Roles of SOX2 and ALDH1A1 in the maintenance of stemness and osimertinib resistance

We further elucidated the roles of SOX2 and ALDH1A1 in stemness and osimertinib resistance through reverse genetic techniques. The small interfering RNA-mediated knockdown of either SOX2 or

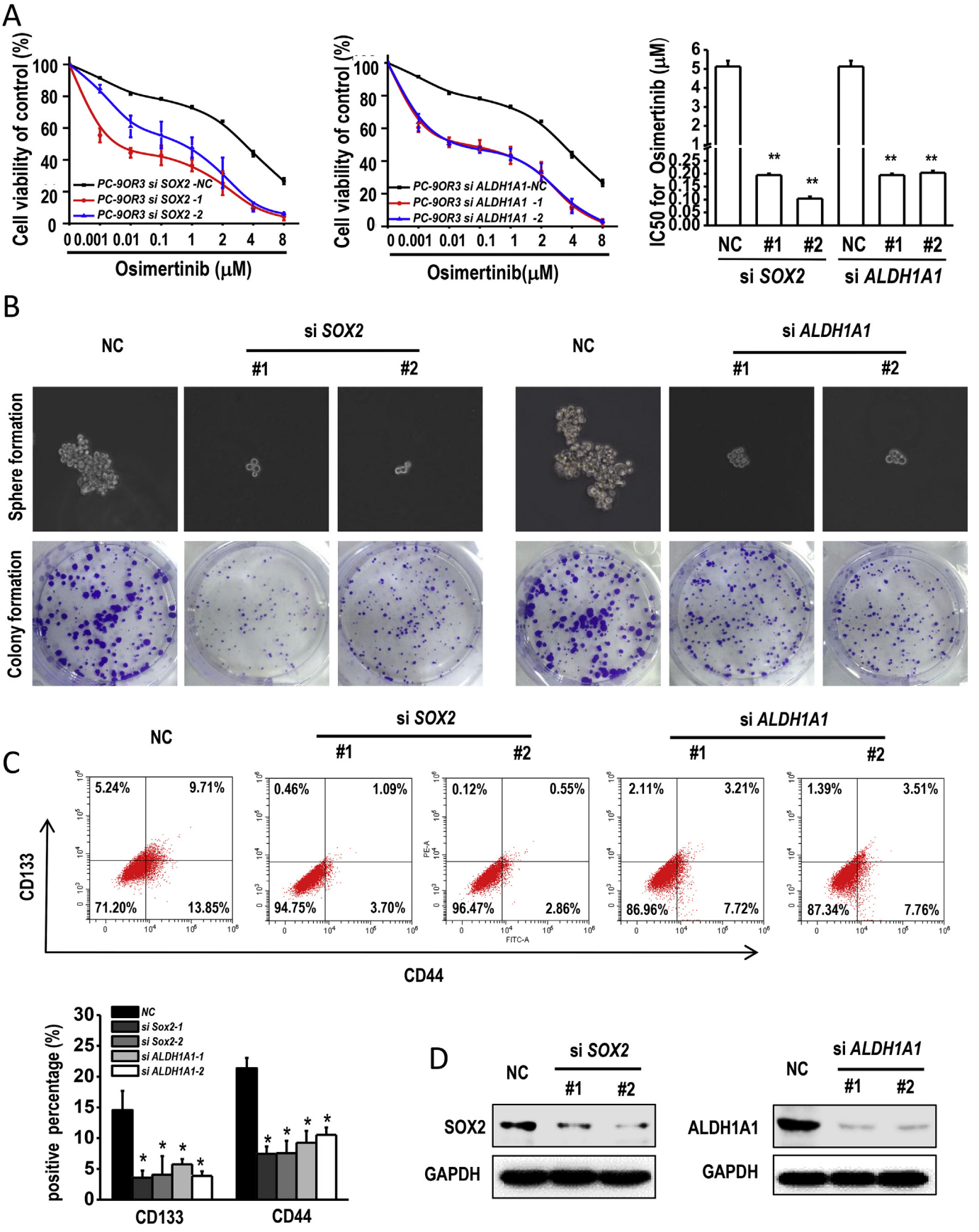

(caption on next page)

Fig. 4. Loss of SOX2 and ALDH1A1 affects osimertinib resistance. (A) Cell viability MTT assay for PC-9OR3 cells transfected with control, *SOX2* and *ALDH1A1* siRNAs, respectively, treated with increasing concentrations of osimertinib for 48 h. Experiments were performed in triplicate, and data are mean ± SEM. Histogram shows IC_{50} values in the indicated groups (**p < 0.01 by Student's *t*-test). (B) Colony formation and pulmosphere formation assays for assessing the PC-9OR3 cell line after transfection with control, *SOX2*, and *ALDH1A1* siRNAs, respectively. (C) CD133/CD44 positive cells were detected by flow cytometry with anti-CD133-FITC and CD44-PE antibodies. The bar chart shows percentages in various groups (n = 3, *p < 0.05 by Student's *t*-test). (D) Western blot showing the expression levels of SOX2 and ALDH1A1 in the PC-9OR3 cell line after transfection with *SOX2* and *ALDH1A1* siRNAs, respectively. GAPDH served as loading control.

ALDH1A1 in PC-9OR3 cells resulted in the re-sensitization of these osimertinib-resistant cells to osimertinib (Fig. 4A and D). Moreover, the knockdown of either SOX2 or ALDH1A1 in PC-9OR3 cells significantly reduced the number and size of pulmospheres compared with controls (Fig. 4B). Consistently, SOX2 or ALDH1A1 knockdown in PC-9OR3 cells significantly decreased colony sizes, suggesting that SOX2 and ALDH1A1 were responsible for the proliferation of osimertinib-resistant cells (Fig. 4B). In addition, the knockdown of either SOX2 or ALDH1A1 in osimertinib-resistant PC-9OR3 cells displayed decreased CD133 + and CD44 $^{+}$ cell populations (Fig. 4C). Overall, these findings suggested that SOX2 and ALDH1A1 are essential in maintaining stemness and resistance to osimertinib.

3.5. Inhibition of autophagy decreased stemness in osimertinib-resistant cells

We next used pharmacologic inhibition of autophagy to explore whether the osimertinib resistance mediated by autophagy involves the maintenance of stemness in the osimertinib-resistant cells. Pulmosphere formation assay revealed that Sp-1 treatment resulted in the formation of smaller spheres in osimertinib-resistant PC-9OR3 cells, compared to vehicle control (Fig. S4). Flow cytometry also revealed that the treatment of both Sp-1 and osimertinib resulted in decreased number of CD133 and CD44 positive population (Fig. 5A), and similar results were obtained with CQ treatment (Fig. S5A). In addition, downregulation of ALDH1A1 and SOX2 protein expression were observed in response to Sp-1 treatment in osimertinib-resistant PC-9OR3 cells, PC-9GROR3 cells and H1975-OR3 cells (Fig. 5B). Interestingly, a more significant downregulation of ALDH1A1 and SOX2 protein expression were observed in response to treatment of both Sp-1 and osimertinib in the osimertinib-resistant cells, as compared to single treatment of either Sp-1 or osimertinib, further implicating ALDH1A1 and SOX2 in osimertinib resistance. Similar results were obtained with CQ treatment (Fig. S5B).

Since Beclin-1 is an important regulation factor of autophagy, we next studied whether knockdown of Beclin-1 may decrease stemness and enhance osimertinib cytotoxicity. Phosphorylated Beclin-1 (Ser 93) were found to be increased in osimertinib-resistant PC-9OR cells, while total Beclin-1 expression remained unchanged (Fig. 5C). siRNA-mediated knockdown of Beclin-1 resulted in enhanced osimertinib cytotoxicity in osimertinib-resistant PC-9OR3 cells (Fig. 5D and E). Furthermore, colony and pulmosphere formation assays, with significant decrease in colony formation and smaller pulmosphere formation in Beclin-1 knockdown cells (Fig. 5F and G), demonstrated that Beclin-1 was important for maintaining stem cell-like properties. In addition, Beclin-1 knockdown also brought about a significant decrease in the number of CD133/CD44-positive cells (Fig. 5H). Moreover, *Beclin-1* knockdown in osimertinib-resistant PC-9OR3 cells resulted in a decrease in SOX2 and ALDH1A1 protein expression (Fig. 5I). Taken together, these results establish the role of autophagy in maintaining stemness to mediate osimertinib resistance.

3.6. Combination of the autophagy inhibitor CQ and osimertinib effectively inhibits the growth of PC-9GR xenografts

Based on the above findings, we next used a PC-9GR xenograft mouse model and further assessed the efficacy of the combination of the autophagy inhibitor CQ and osimertinib in inhibiting cancer cell proliferation. As expected, administration of osimertinib to PC-9GR xenograft mice resulted in significant tumor shrinkage, while treatment of CQ had little effect on tumor size. However, administration of a combination of CQ and osimertinib resulted in a significant tumor shrinkage, compared with osimertinib alone (P < 0.05; Fig. 6A and B). During the entire treatment period, no overt weight loss was observed in mice treated with CQ and/or osimertinib (Fig. 6C).

Through the observations that combined therapy was more effective than monotherapy in PC-9GR xenografts, we further explored the potential mechanism of this efficacy. Osimertinib treatment resulted in significantly increased Beclin-1 phosphorylation and a slight decrease in ALDH1A1 and SOX2 protein expression. On the other hand, combination therapy of osimertinib and CQ resulted in a profound decrease in Beclin-1 phosphorylation and ALDH1A1 and SOX2 expression (Fig. 6D). These findings further suggest that the inclusion of CQ enhanced the therapeutic efficacy of osimertinib *in vivo*, through the inhibition of autophagy and stem cell-like properties.

4. Discussion

Currently, there is no effective approach to overcome resistance to osimertinib. Collective efforts are being done to explore new strategies to overcome osimertinib resistance, such as development of fourth-generation EGFR-TKIs, combination of osimertinib with other agents targeting bypass pathways. Our study provides a new strategy through targeting autophagy to enhance osimertinib cytotoxicity.

Previous reports have implicated autophagy in lung cancer targeted therapy, while results are perplexing [40]. Previously, activation of pro-survival autophagy has been found in therapeutics agents used to treat cancers, and inhibition of autophagy promotes cell death [41–43]. Recently, two studies have reported that osimertinib treatment induced autophagy in lung cancer cells *in vitro* and in xenograft models, while inhibition of autophagy using CQ had little effect on osimertinib sensitivity [23,24]. Therefore, more autophagy inhibitors and siRNA knock-down techniques are needed to inhibit autophagy to further answer the question whether autophagy may control osimertinib cytotoxicity. In the current study, we used several different cell lines and several different autophagy inhibitors. Results from the *in vitro* experiments using osimertinib-resistant cell lines and the tissue samples from patients who had developed osimertinib-resistance have provided evidence that enhanced autophagy potentially contribute to resistance mechanisms to osimertinib. In addition, inhibition of autophagy through both pharmacologic and reverse genetics approach *in vitro* restored osimertinib cytotoxicity. Taken together, our results suggest that enhanced autophagy is involved in decreased osimertinib cytotoxicity and inhibition of autophagy might provide an effective approach to enhance osimertinib cytotoxicity.

How autophagy controls osimertinib cytotoxicity? The heterogeneity of resistance mechanisms found in the osimertinib-resistant cell lines in our current study has prompted us to investigate whether autophagy may decrease osimertinib cytotoxicity through the regulation of stem cell-like properties. We first investigated whether osimertinib-resistant cells exhibit stemness and its potential role in osimertinib resistance. From our observations, osimertinib-resistant cells were found to exhibit stem cell-like properties including enhanced pulmosphere forming ability, high CD133/CD44 enrichment and increased protein expression of stemness factors, SOX2 and ALDH1A1, which were all reversed by the knockdown of SOX2 and ALDH1A1. Several research groups have observed stem cell-like features, including overexpression

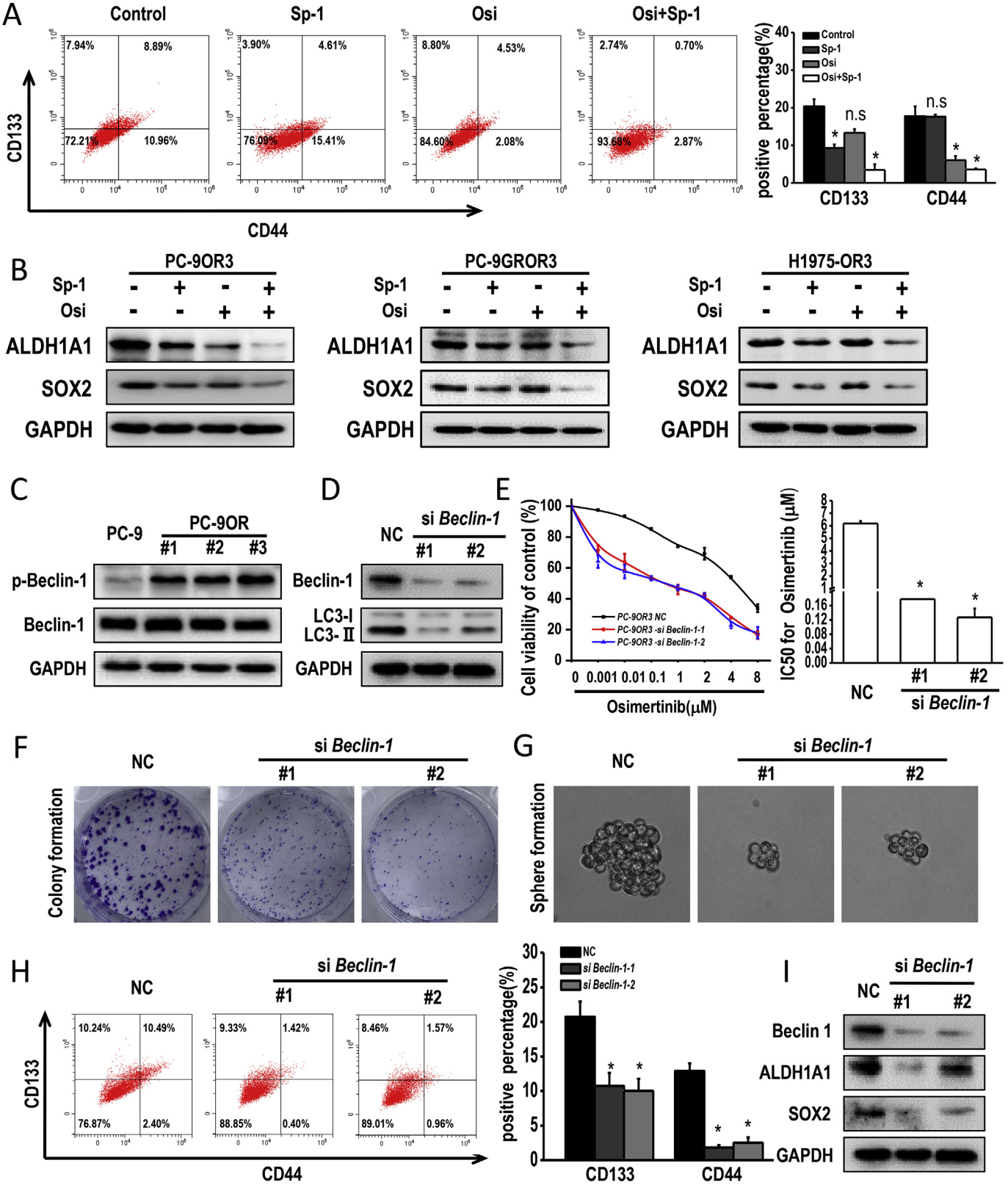

Fig. 5. Autophagy is critical for stem-cell like properties. (A) CD133/CD44 positive cells were detected by flow cytometry with anti-CD133-FITC and CD44-PE antibodies. The bar chart shows percentages in various groups (n = 3, *p < 0.05 by Student's *t*-test). (B) Western blot showing the expression levels of SOX2 and ALDH1A1 in the resistance cells treated with Sp-1 alone or combined with Osi. (C) Phospho-Beclin-1 (Ser93) and total Beclin-1 levels measured by Western blot in parental PC-9 and resistant PC-9OR cells. (D) Western blot showing the expression levels of Beclin-1 and LC3 in the PC-9OR3 cell line after transfection with control and *Beclin-1* siRNAs, respectively. (E) Cell viability of PC-9OR3 cells transfected with control, *Beclin-1* siRNAs. Experiments were performed in triplicate, and data are mean ± SEM. (F) Colony formation for PC-9OR3 cells after transfection with control, *Beclin-1* siRNAs. (G) Pulmosphere formation assays for PC-9OR3 cells after transfection with control, *Beclin-1* siRNAs. (H) CD133/CD44 positive PC-9OR3 cells were detected after transfection with control, *Beclin-1* siRNAs, by flow cytometry with anti-CD133-PITC and CD44-PE antibodies. (I) SOX2 and ALDH1A1 levels were measured in PC-9OR3 cells after transfection with control, *Beclin-1* siRNAs.Sp-1: spautin-1, Osi: osimertinib. GAPDH served as loading control.

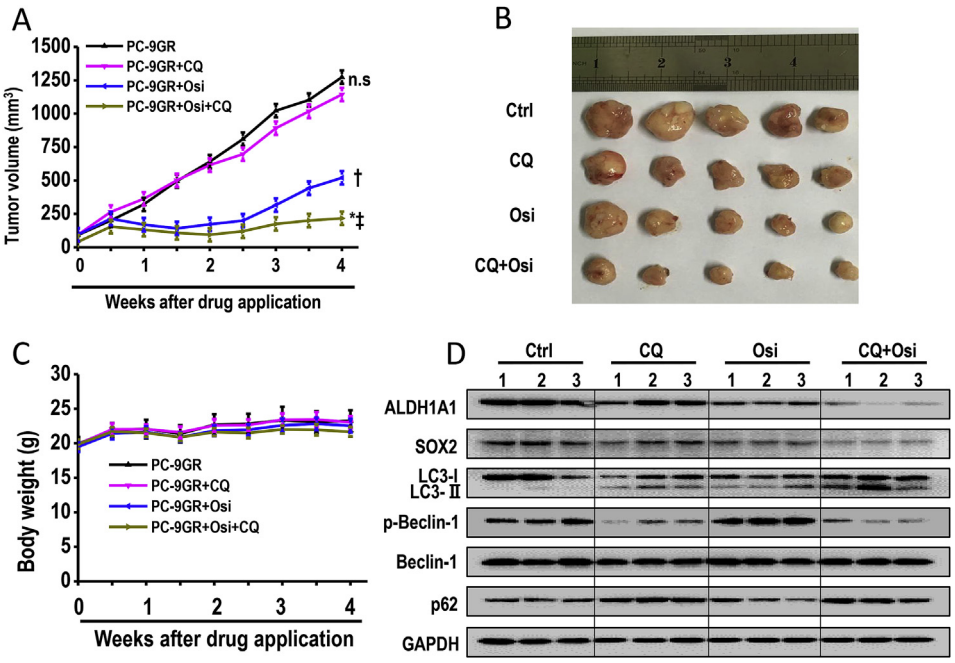

Fig. 6. Combination of the autophagy inhibitor CQ and osimertinib effectively inhibits the growth of PC-9GR xenografts (A) Tumor sizes were presented as mean ± SEM (n = 5); n.s, not significant compared with the control group; *, P < 0.001 compared with the control group; †, P < 0.01 compared with the control group; ‡, P < 0.05 compared with the osimertinib alone group. (B) Macroscopic appearance of PC-9GR xenografts were treated with control, CQ, osimertinib, and combined CQ/osimertinib for 4 weeks. (C) Body weight were presented as mean ± SEM(n = 5). (D) Whole protein cell lysates were prepared randomly from 3 tumors per group for Western blot to detect the indicated proteins.

of putative stem cell markers ALDH1A1 and ABCB1, in cells with acquired resistance to gefitinib or afatinib [44,45]. Furthermore, the stem cell-like characteristics of gefitinib-resistant cells were lost with IL-8 knockdown, resulting in the regain of gefitinib sensitivity [46]. Therefore, our results, together with those previous studies, indicate that enhanced stem cell-like properties mediate osimertinib resistance.

We next investigated the relationship between autophagy and stemness, and found that combination use of osimertinib and autophagy inhibitor could significantly downregulate ALDH1A1 and SOX2 protein expressions and CD133/CD44 positive population in the osimertinib-resistant cells. The possible mechanisms how autophagy regulates stem cell-like characteristics have been reported in several previous studies. Autophagy suppresses hematopoietic stem cell metabolism by clearing active, healthy mitochondria to maintain quiescence and stemness [47]. Autophagy maintains the stemness of ovarian cancer stem cells through regulation of FOXA2 [48], and inhibition of autophagy by ATG5 knock out led to reduction of the $CD44^{+}$ CD117 + cell percentage, as well as decreased chemoresistance and tumorigenic potential of ovarian cancer stem cells [49]. Autophagy promotes the formation of vasculogenic mimicry by glioma stem cells through induction of KDR/VEGFR-2 activation [50]. In acute myeloid leukemia stem cells, autophagy inhibition enhanced sensitivity to BET inhibitor JQ1-induced apoptosis, which was associated with AMPK/ULK1 pathway [51]. In agreement with these reports, our findings indicate that autophagy maintains the stemness of cancer cells, which then contribute to therapeutic resistance.

In addition, inhibition of autophagy through siRNA-mediated knockdown of Beclin-1 resulted in the complete suppression of stem cell-like properties including decreased formation of pulmospheres and reduced levels of the stemness markers SOX2, ALDH1A1, and CD133/CD44. These findings support a new physiological role for macroautophagy in stem-like cell maintenance. Beclin-1 is an important regulator of autophagy, and its phosphorylation at distinct sites has different effect on autophagy [52]. Beclin-1 phosphorylation at Ser93 is essential for activating the pro-autophagic VPS34-BECN1-ATG14 complex [53]. This indicated that autophagy controls osimertinib resistance through regulation of stem cell-like properties, and Beclin-1 played an important role in this process.

More importantly, treatment of xenograft mice with a combination of osimertinib and chloroquine (CQ), an inhibitor of autophagy, markedly decreased tumor growth than treatment with osimertinib alone. CQ is an FDA-approved drug used for malaria, rheumatoid arthritis, and other autoimmune diseases. It is very cheap and has an established history of good tolerability. Currently, there are a number of clinical trials testing the efficacy of CQ in various types of cancer (http://clinicaltrials.gov). Combination use of osimertinib and CQ may deserve further exploration in NSCLC therapy.

The current study has several limitations. First, xenograft model experiments were only performed in osimertinib-sensitive cells, and more works are needed in the future to study whether autophagy inhibition may decrease tumor growth in mouse xenografts based on osimertinib-resistant cells. Second, paired tumor tissues before and after osimertinib resistance were obtained from only 5 patients, and more clinical works are needed in the future.

In summary, our study is the first to elucidate a previously unknown mechanism by which autophagy decreases osimertinib cytotoxicity. These findings are critical for developing potential therapeutic strategy to enhance osimertinib cytotoxicity. Further clinical studies are needed to assess autophagy levels in osimertinib-resistant patients and to test the efficacy of autophagy inhibition in combination with osimertinib in *EGFR*-mutant patients.

Conflicts of interest

The authors declare no potential conflicts of interest.

Declarations of interest

None.

Acknowledgments

This work was supported by the Natural Science Foundation of China (81672284, 81472189, 81672287, 81702288 and 81702291) and a foundation for PLA Young Scientists (16QNP106). We thank Prof. Xiang Xu and Prof. Xueqing Xu (both from Army Medical University) for their kind advice about design of the study and Dr. Analyn Lizaso of Burning Rock Biotech for improving the language and data interpretation of the manuscript.

Appendix A. Supplementary data

Supplementary data to this article can be found online at https://doi.org/10.1016/j.canlet.2019.03.027.

References

[1] T.S. Mok, Y.L. Wu, M.J. Ahn, M.C. Garassino, H.R. Kim, S.S. Ramalingam, et al., Investigators, osimertinib or platinum-pemetrexed in EGFR T790M-positive lung cancer, N. Engl. J. Med. 376 (2017) 629–640.

[2] F. Skoulidis, V.A. Papadimitrakopoulou, Targeting the gatekeeper: osimertinib in EGFR T790M mutation-positive non-small cell lung cancer, Clin. Cancer Res. 23 (2017) 618–622.

[3] W. Pao, V.A. Miller, K.A. Politi, G.J. Riely, R. Somwar, M.F. Zakowski, et al., Acquired resistance of lung adenocarcinomas to gefitinib or erlotinib is associated with a second mutation in the EGFR kinase domain, PLoS Med. 2 (2005) e73.

[4] H.A. Yu, M.E. Arcila, N. Rekhtman, C.S. Sima, M.F. Zakowski, W. Pao, et al., Analysis of tumor specimens at the time of acquired resistance to EGFR-TKI therapy in 155 patients with EGFR-mutant lung cancers, Clin. Cancer Res. 19 (2013) 2240–2247.

[5] J.C. Soria, Y. Ohe, J. Vansteenkiste, T. Reungwetwattana, B. Chewaskulyong, K.H. Lee, et al., Investigators, osimertinib in untreated EGFR-mutated advanced non-small-cell lung cancer, N. Engl. J. Med. 378 (2018) 113–125.

[6] P.A. Janne, J.C. Yang, D.W. Kim, D. Planchard, Y. Ohe, S.S. Ramalingam, et al., AZD9291 in EGFR inhibitor-resistant non-small-cell lung cancer, N. Engl. J. Med. 372 (2015) 1689–1699.

[7] K.S. Thress, C.P. Paweletz, E. Felip, B.C. Cho, D. Stetson, B. Dougherty, et al., Acquired EGFR C797S mutation mediates resistance to AZD9291 in non-small cell lung cancer harboring EGFR T790M, Nat. Med. 21 (2015) 560–562.

[8] J.J. Chabon, A.D. Simmons, A.F. Lovejoy, M.S. Esfahani, A.M. Newman, H.J. Haringsma, et al., Circulating tumour DNA profiling reveals heterogeneity of EGFR inhibitor resistance mechanisms in lung cancer patients, Nat. Commun. 7 (2016) 11815.

[9] T.M. Kim, A. Song, D.W. Kim, S. Kim, Y.O. Ahn, B. Keam, et al., Mechanisms of acquired resistance to AZD9291: a mutation-selective, irreversible EGFR inhibitor, J. Thorac. Oncol. 10 (2015) 1736–1744.

[10] D. Planchard, Y. Loriot, F. Andre, A. Gobert, N. Auger, L. Lacroix, et al., EGFR-independent mechanisms of acquired resistance to AZD9291 in EGFR T790M-positive NSCLC patients, Ann. Oncol. 26 (2015) 2073–2078.

[11] S. Ortiz-Cuaran, M. Scheffler, D. Plenker, L. Dahmen, A.H. Scheel, L. Fernandez-Cuesta, et al., Heterogeneous mechanisms of primary and acquired resistance to third-generation EGFR inhibitors, Clin. Cancer Res. 22 (2016) 4837–4847.

[12] H. Mizuuchi, K. Suda, I. Murakami, K. Sakai, K. Sato, Y. Kobayashi, et al., Oncogene swap as a novel mechanism of acquired resistance to epidermal growth factor receptor-tyrosine kinase inhibitor in lung cancer, Cancer Sci. 107 (2016) 461–468.

[13] C.A. Eberlein, D. Stetson, A.A. Markovets, K.J. Al-Kadhimi, Z. Lai, P.R. Fisher, et al., Acquired resistance to the mutant-selective EGFR inhibitor AZD9291 is associated with increased dependence on RAS signaling in preclinical models, Cancer Res. 75 (2015) 2489–2500.

[14] S. Nukaga, H. Yasuda, K. Tsuchihara, J. Hamamoto, K. Masuzawa, I. Kawada, et al., Amplification of EGFR wild-type Alleles in non-small cell lung cancer cells confers acquired resistance to mutation-selective EGFR tyrosine kinase inhibitors, Cancer Res. 77 (2017) 2078–2089.

[15] L. Yu, Y. Chen, S.A. Tooze, Autophagy pathway: cellular and molecular mechanisms, Autophagy 14 (2017) 207–215.

[16] BRAF inhibitor resistance can be overcome by blocking autophagy, Cancer Discov. 4 (2014) OF10.

[17] P. Auberger, A. Puissant, Autophagy, a key mechanism of oncogenesis and resistance in leukemia, Blood 129 (2017) 547–552.

[18] Z. Chen, A.E. Teo, N. McCarty, ROS-induced CXCR4 signaling regulates mantle cell lymphoma (MCL) cell survival and drug resistance in the bone marrow microenvironment via autophagy, Clin. Cancer Res. 22 (2016) 187–199.

[19] Y. Wei, Z. Zou, N. Becker, M. Anderson, R. Sumpter, G. Xiao, et al., EGFR-mediated Beclin 1 phosphorylation in autophagy suppression, tumor progression, and tumor chemoresistance, Cell 154 (2013) 1269–1284.

[20] Z. Wang, T. Du, X. Dong, Z. Li, G. Wu, R. Zhang, Autophagy inhibition facilitates erlotinib cytotoxicity in lung cancer cells through modulation of endoplasmic reticulum stress, Int. J. Oncol. 48 (2016) 2558–2566.

[21] X. Hu, S. Shi, H. Wang, X. Yu, Q. Wang, S. Jiang, et al., Blocking autophagy improves the anti-tumor activity of afatinib in lung adenocarcinoma with activating EGFR mutations in vitro and in vivo, Sci. Rep. 7 (2017) 4559.

[22] Y. Chen, E.S. Henson, W. Xiao, D. Huang, E.M. McMillan-Ward, S.J. Israels, et al., Tyrosine kinase receptor EGFR regulates the switch in cancer cells between cell survival and cell death induced by autophagy in hypoxia, Autophagy 12 (2016) 1029–1046.

[23] Z. Zhang, M. Zhang, H. Liu, W. Yin, AZD9291 promotes autophagy and inhibits PI3K/Akt pathway in NSCLC cancer cells, J. Cell. Biochem. 120 (2019) 756–767.

[24] Z.H. Tang, W.X. Cao, M.X. Su, X. Chen, J.J. Lu, Osimertinib induces autophagy and apoptosis via reactive oxygen species generation in non-small cell lung cancer cells, Toxicol. Appl. Pharmacol. 321 (2017) 18–26.

[25] Z. Yao, S. Fenoglio, D.C. Gao, M. Camiolo, B. Stiles, T. Lindsted, et al., TGF-beta IL-6 axis mediates selective and adaptive mechanisms of resistance to molecular targeted therapy in lung cancer, Proc. Natl. Acad. Sci. U. S. A. 107 (2010) 15535–15540.

[26] A.M. Newman, A.F. Lovejoy, D.M. Klass, D.M. Kurtz, J.J. Chabon, F. Scherer, et al., Integrated digital error suppression for improved detection of circulating tumor DNA, Nat. Biotechnol. 34 (2016) 547–555.

[27] E.N. N'Diaye, K.K. Kajihara, I. Hsieh, H. Morisaki, J. Debnath, E.J. Brown, PLIC proteins or ubiquilins regulate autophagy-dependent cell survival during nutrient starvation, EMBO Rep. 10 (2009) 173–179.

[28] J.M. Gump, L. Staskiewicz, M.J. Morgan, A. Bamberg, D.W. Riches, A. Thorburn, Autophagy variation within a cell population determines cell fate through selective degradation of Fap-1, Nat. Cell Biol. 16 (2014) 47–54.

[29] L. Li, R. Han, H. Xiao, C. Lin, Y. Wang, H. Liu, et al., Metformin sensitizes EGFR-TKI-resistant human lung cancer cells in vitro and in vivo through inhibition of IL-6 signaling and EMT reversal, Clin. Cancer Res. 20 (2014) 2714–2726.

[30] S.K. Yeo, J. Wen, S. Chen, J.L. Guan, Autophagy differentially regulates distinct breast cancer stem-like cells in murine models via EGFR/Stat3 and tgfbeta/smad signaling, Cancer Res. 76 (2016) 3397–3410.

[31] S.M. Ou, C.J. Shih, P.W. Chao, H. Chu, S.C. Kuo, Y.J. Lee, et al., Effects on clinical outcomes of adding dipeptidyl peptidase-4 inhibitors versus sulfonylureas to metformin therapy in patients with type 2 diabetes mellitus, Ann. Intern. Med. 163 (2015) 663–672.

[32] S. Sarvi, A.C. Mackinnon, N. Avlonitis, M. Bradley, R.C. Rintoul, D.M. Rassl, et al., CD133+ cancer stem-like cells in small cell lung cancer are highly tumorigenic and chemoresistant but sensitive to a novel neuropeptide antagonist, Cancer Res. 74 (2014) 1554–1565.

[33] K. Okudela, T. Woo, H. Mitsui, M. Tajiri, M. Masuda, K. Ohashi, Expression of the potential cancer stem cell markers, CD133, CD44, ALDH1, and beta-catenin, in primary lung adenocarcinoma–their prognostic significance, Pathol. Int. 62 (2012) 792–801.

[34] M. Nishino, M. Ozaki, A.E. Hegab, J. Hamamoto, S. Kagawa, D. Arai, et al., Variant CD44 expression is enriching for a cell population with cancer stem cell-like characteristics in human lung adenocarcinoma, J. Cancer 8 (2017) 1774–1785.

[35] W. Sterlacci, S. Savic, M. Fiegl, E. Obermann, A. Tzankov, Putative stem cell markers in non-small-cell lung cancer: a clinicopathologic characterization, J. Thorac. Oncol. 9 (2014) 41–49.

[36] V. Justilien, M.P. Walsh, S.A. Ali, E.A. Thompson, N.R. Murray, A.P. Fields, The PRKCI and SOX2 oncogenes are coamplified and cooperate to activate Hedgehog signaling in lung squamous cell carcinoma, Canc. Cell 25 (2014) 139–151.

[37] S. Akunuru, Q. James Zhai, Y. Zheng, Non-small cell lung cancer stem/progenitor cells are enriched in multiple distinct phenotypic subpopulations and exhibit plasticity, Cell Death Dis. 3 (2012) e352.

[38] I. Dogan, S. Kawabata, E. Bergbower, J.J. Gills, A. Ekmekci, W. Wilson, et al., SOX2 expression is an early event in a murine model of EGFR mutant lung cancer and promotes proliferation of a subset of EGFR mutant lung adenocarcinoma cell lines, Lung Canc. 85 (2014) 1–6.

[39] I.G. Kim, S.Y. Kim, S.I. Choi, J.H. Lee, K.C. Kim, E.W. Cho, Fibulin-3-mediated inhibition of epithelial-to-mesenchymal transition and self-renewal of ALDH+ lung cancer stem cells through IGF1R signaling, Oncogene 33 (2014) 3908–3917.

[40] E. Henson, Y. Chen, S. Gibson, EGFR family members' regulation of autophagy is at a crossroads of cell survival and death in cancer, Cancers (Basel) 9 (2017).

[41] J. Han, W. Hou, L.A. Goldstein, C. Lu, D.B. Stolz, X.M. Yin, et al., Involvement of protective autophagy in TRAIL resistance of apoptosis-defective tumor cells, J. Biol. Chem. 283 (2008) 19665–19677.

[42] L. Amrein, D. Soulieres, J.B. Johnston, R. Aloyz, p53 and autophagy contribute to dasatinib resistance in primary CLL lymphocytes, Leuk. Res. 35 (2011) 99–102.

[43] M.H. Lee, D. Koh, H. Na, N.L. Ka, S. Kim, H.J. Kim, et al., MTA1 is a novel regulator of autophagy that induces tamoxifen resistance in breast cancer cells, Autophagy (2017) 0.

[44] S. Hashida, H. Yamamoto, K. Shien, Y. Miyoshi, T. Ohtsuka, K. Suzawa, et al., Acquisition of cancer stem cell-like properties in non-small cell lung cancer with acquired resistance to afatinib, Cancer Sci. 106 (2015) 1377–1384.

[45] K. Shien, S. Toyooka, H. Yamamoto, J. Soh, M. Jida, K.L. Thu, et al., Acquired resistance to EGFR inhibitors is associated with a manifestation of stem cell-like properties in cancer cells, Cancer Res. 73 (2013) 3051–3061.

[46] Y.N. Liu, T.H. Chang, M.F. Tsai, S.G. Wu, T.H. Tsai, H.Y. Chen, et al., IL-8 confers resistance to EGFR inhibitors by inducing stem cell properties in lung cancer, Oncotarget 6 (2015) 10415–10431.

[47] T.T. Ho, M.R. Warr, E.R. Adelman, O.M. Lansinger, J. Flach, E.V. Verovskaya, et al., Autophagy maintains the metabolism and function of young and old stem cells, Nature 543 (2017) 205–210.

[48] Q. Peng, J. Qin, Y. Zhang, X. Cheng, X. Wang, W. Lu, et al., Autophagy maintains the stemness of ovarian cancer stem cells by FOXA2, J. Exp. Clin. Cancer Res. : CR (Clim. Res.) 36 (2017) 171.

[49] A. Pagotto, G. Pilotto, E.L. Mazzoldi, M.O. Nicoletto, S. Frezzini, A. Pasto, et al., Autophagy inhibition reduces chemoresistance and tumorigenic potential of human ovarian cancer stem cells, Cell Death Dis. 8 (2017) e2943.

[50] H.B. Wu, S. Yang, H.Y. Weng, Q. Chen, X.L. Zhao, W.J. Fu, et al., Autophagy-induced KDR/VEGFR-2 activation promotes the formation of vasculogenic mimicry by glioma stem cells, Autophagy 13 (2017) 1528–1542.

[51] J.E. Jang, J.I. Eom, H.K. Jeung, J.W. Cheong, J.Y. Lee, J.S. Kim, et al., AMPK-ULK1-Mediated autophagy confers resistance to BET inhibitor JQ1 in acute myeloid leukemia stem cells, Clin. Cancer Res. 23 (2017) 2781–2794.

[52] M.B. Menon, S. Dhamija, Beclin 1 phosphorylation - at the center of autophagy regulation, Front. Cell Dev. Biol. 6 (2018) 137.

[53] J. Kim, Y.C. Kim, C. Fang, R.C. Russell, J.H. Kim, W. Fan, et al., Differential regulation of distinct Vps34 complexes by AMPK in nutrient stress and autophagy, Cell 152 (2013) 290–303.